Construction and Building Materials 123 (2016) 214–225

Contents lists available at ScienceDirect

Construction and Building Materials

journal homepage: www.elsevier.com/locate/conbuildmat

Ground-penetrating radar for observing tree trunks and other cylindrical objects

Jana Ježová *, Laurence Mertens, Sébastien Lambot

Université catholique de Louvain, Louvain-la-Neuve, Belgium

HIGHLIGHTS

- Analysis of radar wave propagation in tree trunk.
- Numerical, laboratory and real tree radar data.
- Significant effects of the total internal reflection.
- Visualisation of the electric field distribution in the trunk using Finite-Difference Time-Domain (gprMax2D).

ARTICLE INFO

Article history:
Received 1 October 2015
Received in revised form 24 June 2016
Accepted 5 July 2016

Keywords:
Ground-penetrating radar
Non-destructive testing
Total internal reflection
Tree trunk
Wood
Column

ABSTRACT

To improve forest management and to prevent collapses of trees, it is necessary to investigate the internal part of tree trunks. In order to do it non-invasively, ground-penetrating radar (GPR) appears as a promising inspection device. The objective of this paper is to investigate particularities of tree trunks radar images, considering the circumferential data acquisition geometry, as a function of the radar configuration and trunk section structures. In order to better understand this kind of data, a target reflection curve was analytically described, then, the total internal reflection (TIR) phenomenon was explained and illustrated. Subsequently, classical radar measurements were compared with an application of differently shaped (planar and circular) metal shields acting as perfect electrical conductors (PEC). For comparing the methods, three experiments were performed: (1) numerical simulations using the software gprMax2D, based on Finite-Difference Time-Domain method, (2) GPR investigation of a laboratory model of a tree trunk, (3) real tree trunk measurements. The use of a planar or circular PEC increased the visibility of the medium edges, so, these GPR images were considered of a better quality. Internal object reflection curve and TIR detection were essential for general description of a GPR image. All experiments showed satisfactorily the internal inhomogeneity and the information will be useful for future tomographic reconstruction.

1. Introduction

Trees are everyday part of human life and therefore it is important to pay attention to their conditions, as they are constantly endangered by natural defects and biological degradation. In industry, it is necessary to detect flaws in wood (knots, cracks, reaction wood, etc.) before its use as a building material (beam, columns, etc.), furniture or musical instruments. In urban areas or around roads, it is highly important to prevent collapses of trees, which can lead to injuries and damages.

From the macroscopic aspect, the healthy tree trunk internal structure is divided into three main parts: heartwood, sapwood and bark [1,2]. These different parts are very anisotropic and heterogeneous [3–6]. Some flaws are visible on the bark, whereas others are hidden in the inner part of the trunk, which can be investigated invasively or non-invasively. Typical example of destructive inspection is core drilling or in an extreme case chopping down of the tree. In order to avoid destruction of valuable trees, it is usually recommended to use non-invasive methods for the evaluation of the state of the trunk.

There are several techniques for non-invasive investigation of tree trunks. A review of methods for wood testing is described in [7]. Nicolotti et al. [8] and Sambuelli et al. [9] compared three technologies for tree trunk inspection: ultrasonic, electrical resistivity and ground-penetrating radar (GPR) tomography. The most popular approach for trunk examination is the ultrasonic tomography, which is based on propagation of elastic waves through the trunk

* Corresponding author.
E-mail address: jana.jezova@uclouvain.be (J. Ježová).

http://dx.doi.org/10.1016/j.conbuildmat.2016.07.005

and determination of the wave velocity distribution [10]. The electrical resistivity tomography is also used and consists in injecting electrical currents into the trunk using a specific electrode configuration. Potential differences are then measured in order to reconstruct the section resistivity distribution using inversion [11].

GPR is based on scattering of electromagnetic waves that are radiated from a transmitting antenna [12,13]. The waves propagate through the medium, and when they come across an electromagnetic contrast, a part of the field is reflected and recorded by a receiving antenna [14]. GPR has been used in many different fields [15], such as civil engineering [16,17], protection of cultural heritage [18], transport engineering [19], soil moisture mapping [20,21], and it is increasingly used for observation of wooden samples and tree trunks. In [22–25] the authors analysed anisotropy of wood using GPR and reported that its dielectric properties are strongly dependent on the grain orientation (longitudinal arrangement of wood fibres). GPR has also been used for inspection of the internal structure of wooden beams [26]. In [27,8,28,29] it was used for imaging living tree trunks with 900, 1000 and 1500 MHz centre frequency antennas, respectively. Measurements were performed using circumferential and also vertical sensing along the trunk. The reflection mode (transmitter and receiver within the same box) and a transmission mode (separate transmitting and receiving antennas) were used. Lorenzo et al. [29] used a metal shield for an estimation of average permittivity of tree trunks. All authors have shown that the electromagnetic contrast between external and internal zones of a trunk causes strong reflections. In practice, the antenna should be always in a good contact with the bark, because air gaps between the antenna and the bark lead to degradation of the radar image.

In particular, tree trunk GPR data analysis is complex because of the circular shape, the inner structure, anisotropy (grain orientation) and the dependence of the wood electromagnetic properties on water content (which can range from about 30% to more than 200% of weight of wood substance for a living trunk [30]), density, temperature and on the frequency of the applied field [31–33]. In addition, weak dielectric contrasts amongst the healthy and decayed wood may not always allow for proper delineation of the decayed zone [28]. The operating frequency range also determines the resolution of the radar image. Because of relatively high attenuation and associated shallow penetration of the waves into the wood, it is recommended to use an antenna with a centre frequency of maximum 1 GHz [29]. In that respect, microwave sensing of tree trunks is also limited by the stem diameter. Indeed, due to the limited wave penetration depth, it is not straightforward to investigate large trees (e.g., with a diameter larger than 1 m). Notwithstanding the use of GPR for tree trunk imaging is a complex problem, it presents the advantages of being quicker and providing better resolution than the above-mentioned investigation methods. In the future applications, GPR imaging will involve inverse tomographic reconstruction (see [27]). An important step in tree trunk radar imaging is the reconstruction of the echoes following the circular shape of the trunk from the peripheral acquisitions. In particular, the multiples occurring after the opposite side echoes should be eliminated. Similar investigation performed on a pedestal of a monument was also done by Bonomo et al. [34]. The essential preliminary step is to select from GPR images the part of the signal representing wood when using reflection mode, hence it is necessary to detect the edge of the opposite side of the tree trunk.

The objective of this study is to investigate particular features occurring in tree trunk radar images, due to the circumferential data acquisition geometry, as a function of the radar configuration and trunk section structures. In particular, we considered (1) common zero-offset reflection imaging, (2) reflection imaging including a planar perfect electrical conductor (PEC), and (3) reflection imaging including a PEC arc. In that respect, numerical, laboratory and real tree trunk experiments were performed. The programme gprMax2D [35], a numerical model based on the Finite-Difference Time-Domain (FDTD) method [36], was used for the numerical analyses. Then, a cylindrical model including PVC, paper and sand, was built and tested in the laboratory. Finally, a real tree trunk was investigated. Furthermore, we characterized analytically the shape of a reflection curve of a circular inhomogeneity hidden in the cylindrical medium during circumferential data acquisition for easier determination of the position, shape and size of the observed internal target. Moreover, the influence of the total internal reflection (TIR) was described and analysed. The analytical reflection curve and the TIR were validated on simulated GPR data using gprMax2D and on the laboratory GPR data.

2. Reflection curve equation

Considering a circumferential GPR data acquisition rather than planar, as commonly dealt with in GPR applications, it is necessary to consider the different analytical expressions of the reflection curve corresponding to a local heterogeneity. Unlike the traditional hyperbola appearing during a planar data acquisition, in the case of circumferential measurement the reflection shape is different. Using the straight-ray approximation, for a regular circle with a circular target inside (Fig. 1) it is possible to analytically describe the target reflection curves for different initial antenna position around the trunk. In order to get the equation of the curves, one starts from Eqs. (1) and (2), where v is the velocity of waves in the medium (m/s), c is the speed of light in free space (m/s), ε_{r1} is the relative permittivity of the medium (dimensionless), t is the propagation time of the waves (s), and d is the distance from the antenna to the target (m):

$$v = \frac{c}{\sqrt{\varepsilon_{r1}}} \quad (1)$$

$$t = \frac{2 \cdot d}{v} \quad (2)$$

The distance d (see Fig. 1) can be expressed by Eq. (3), where (p_x, p_y) are the coordinates of the position of the antenna (m), (x_2, y_2) are the coordinates of the target centre (m), and R_2 is the radius of the target (m).

$$d = \sqrt{(p_x - x_2)^2 + (p_y - y_2)^2} - R_2 \quad (3)$$

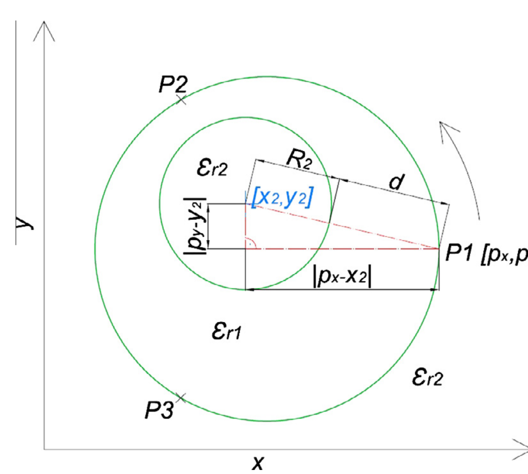

Fig. 1. Straight-ray circular model configuration.